

Formation of Aromatum Chaos, Mars: Morphological development as a result of volcano-ice interactions

Harald J. Leask,¹ Lionel Wilson,¹ and Karl L. Mitchell^{1,2}

Received 3 August 2005; revised 10 May 2006; accepted 16 May 2006; published 17 August 2006.

[1] Morphological examination of the Aromatum Chaos depression on Mars supports earlier suggestions that it is a site of cryosphere disruption and release of pressurized water trapped in an underlying aquifer. We infer that the cause of cryosphere disruption was intrusion of a volcanic sill, confined laterally by earlier intruded dikes, and consequent melting of ice by heat from the sill. The vertical extents and displacements of blocks of terrain on the floor of the depression, together with an estimate of the cryosphere thickness, constrain the vertical extent of ice melting and hence the thickness of the sill (~ 100 m) and the depth at which it was intruded ($\sim 2\text{--}5$ km). At least $\sim 75\%$ of the volume of material removed from Aromatum Chaos must have been crustal rock rather than melted ice. Water from melted cryosphere ice played a negligible role in creating the depression, the process being dominated by released aquifer water. For sediment loads of 30–40% by volume, 10,500–16,500 km³ of aquifer water must have passed through the depression to carry away rock as entrained sediment and erode the associated Ravi Vallis channel. These required water volumes are 2–3 times larger than the amount of water that could reasonably be contained in aquifers located beneath the area of incipiently collapsed ground to the west of Aromatum Chaos and suggest a much larger water source. Given that this source probably also fed the nearby Shalbatana Vallis outflow channel, Gangis Chasma is the most likely candidate.

Citation: Leask, H. J., L. Wilson, and K. L. Mitchell (2006), Formation of Aromatum Chaos, Mars: Morphological development as a result of volcano-ice interactions, *J. Geophys. Res.*, *111*, E08071, doi:10.1029/2005JE002549.

1. Introduction

[2] Key factors shaping the history of Mars are the long-term presence of H₂O near the surface and the fact that Mars has been volcanically active throughout its life [Theilig and Greeley, 1979]. The interactions between the volcanic and hydrological systems have produced numerous surface features [e.g., Squires et al., 1987; McKenzie and Nimmo, 1999; Head and Wilson, 2001; Burr et al., 2002a, 2002b, 2002c; Wilson and Mouginis-Mark, 2003; Burr, 2003; Head et al., 2003], the morphological properties of which allow investigation of the mechanisms of those interactions. One such example occurs at the depression Aromatum Chaos, which is clearly the source of the outflow channel system Ravi Vallis, located in Xanthe Terra (Figure 1) at 1.1°S, 317.0°E (U.S. Geological Survey, Gazetteer of Planetary Nomenclature, available at <http://planetarynames.wr.usgs.gov/>). Aromatum Chaos is 91.5 km in greatest extent, orientated roughly northeast-southwest (Figure 2) and averages ~ 30 km at right angles to this direction. It has

previously been suggested that Aromatum Chaos is the site of an interaction between the cryosphere, the hydrosphere and volcanic intrusions [Coleman, 2003].

[3] We concur with this general idea, but it is our contention that the details of the morphology of Aromatum Chaos specifically suggest that the intrusion of a sill was the essential element in triggering its formation and subsequent evolution [Leask et al., 2004; Leask, 2005], and we attempt to test this proposal as follows. We examine the morphology of the Aromatum Chaos depression in the maximum possible detail using altimetry from the Mars Orbiter Laser Altimeter (MOLA) instrument on Mars Global Surveyor (MGS) and imaging data from the Mars Orbiter Camera (MOC) on MGS and the Thermal Emission Imaging Spectrometer (THEMIS) instrument on Mars Odyssey. We investigate possible structural control of the collapsed features on the floor of the depression which could be linked to structurally controlled features in the vicinity. We also determine the volume of material missing from the depression and, by considering the ratio of ice to rock in this material [Hanna and Philips, 2003, 2005], assess the separate volumes of these components. Thermal calculations and geometric constraints are used to estimate the maximum sill thickness and the timescale for initiation of water release from a deep aquifer as the presence of the sill destabilizes the cryosphere. Finally, by making reasonable assumptions about the ability of the water from the aquifer to carry suspended solids while rising through the fractures

¹Planetary Science Research Group, Environmental Science Department, Institute of Environmental and Natural Sciences, Lancaster University, Lancaster, UK.

²Now at Jet Propulsion Laboratory, Pasadena, California, USA.

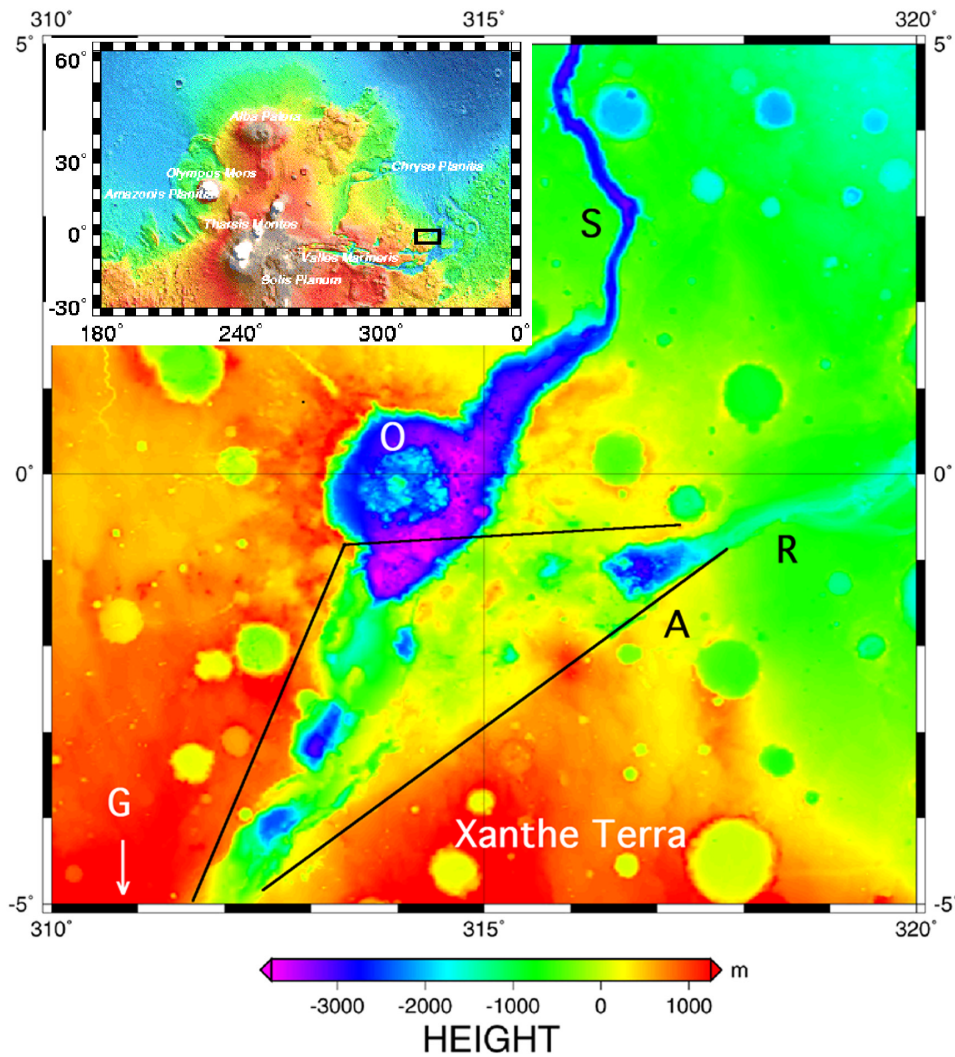


Figure 1. Topography (gridded MOLA data) of Xanthe Terra region, Mars, showing Aromatum Chaos (A), Ravi Vallis (R), Shalbatana Vallis (S), and Orson Welles Crater (O). Solid lines define the area that is the likely location of the aquifer system feeding Aromatum Chaos. The source of the water for the aquifer system was Gangis Chasma, which is located just to the south of the area shown, indicated by the arrow and the letter G. Inset shows location of study area.

beneath the depression, and subsequently flowing upward and laterally through the depression itself, we estimate the minimum volume of water that must have overflowed from Aromatum Chaos into the associated Ravi Vallis.

2. Regional Context of Aromatum Chaos

[4] The Aromatum Chaos depression (Figure 2) is located in the Xanthe Terra region of Mars, in highland terrain close to the highland-lowland dichotomy boundary. Large areas of Xanthe Terra have been affected by subsidence and collapse (Figure 1). The area has been more deeply dissected locally by the outflow channels Shalbatana Vallis and Ravi Vallis and their source areas. A former impounded ice-covered lake in Gangis Chasma has been proposed as the main source for the water passing through the subsurface of Xanthe Terra to form both of these systems [Cabrol *et al.*, 1997; Kuzmin *et al.*, 2002; Palmero *et al.*, 2003; Rodriguez *et al.*, 2003; Coleman, 2002, 2004].

[5] The formation of the outflow channel at Shalbatana Vallis and the subsequent drainage system of Gangis Chasma is thought by Scott and Tanaka [1986] (as discussed by Nelson and Greeley [1999]) and Nelson and Greeley [1999] to have started during the Early Hesperian, and ended between the Late Hesperian and Early Amazonian. Rotto and Tanaka [1995] (as discussed by Kuzmin *et al.* [2002]) show that channel deposits at Shalbatana Vallis, which were associated with catastrophic floods, may have occurred from the Hesperian up to the Early Amazonian. However, Rodriguez *et al.* [2003] estimated that Shalbatana Vallis may have begun to form earlier, between the Late Noachian and the Early Hesperian, and Kuzmin *et al.* [2002] suggest that some water erosion and deposition in Shalbatana Vallis may have occurred as recently as the Late Amazonian.

[6] The area immediately to the west of Aromatum Chaos shows clear evidence of fracturing and pitting, with a noticeable elongate area of collapse to the southwest, which

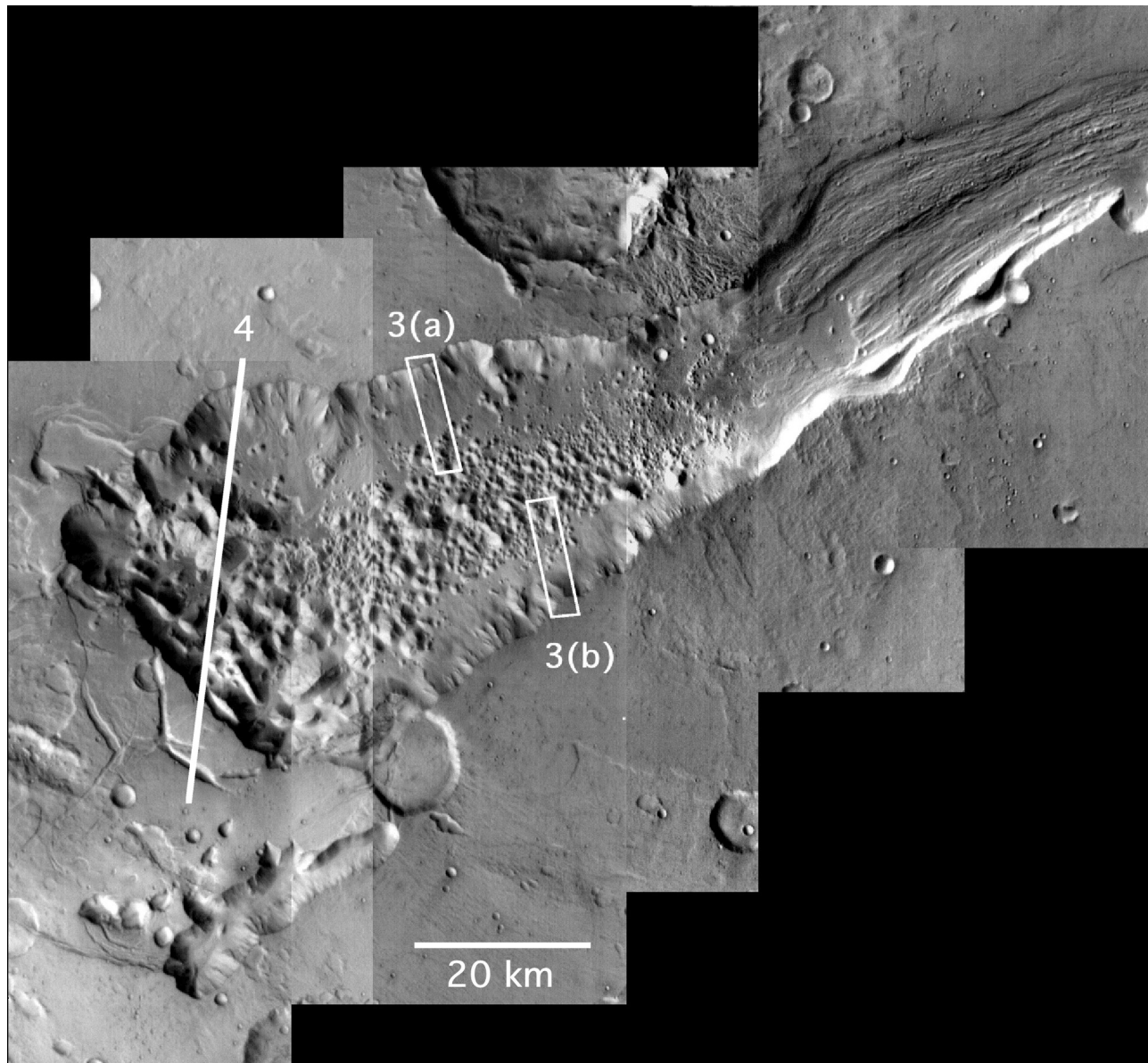


Figure 2. Mosaic of THEMIS (VIS) images of Aromatum Chaos depression (left) and upstream part of Ravi Vallis (right). Locations of Figures 3a and 3b are shown. Mosaic bounded by 0.11°S and 2.11°S and 316.24°E and 318.50°E . North is to the top. White line is location of profile shown in Figure 4.

reaches a depth of about 1 km (Figure 1). There appears to have been hardly any disturbance of the surface to the south and southeast of Aromatum Chaos, and very little disturbance to the north. Furthermore, the boundaries of the Aromatum Chaos depression have many near-linear segments (Figure 2), and this strongly suggests that dike intrusions have been a factor in controlling the location of the depression and in limiting the major collapse to the interior of the region that they define. This would be particularly easy to understand if the dikes had maintained enough structural integrity to act as impervious obstacles to lateral subsurface water flow.

[7] THEMIS images show that ejecta from the Dia-Cau impact crater, which is located at 0.4°S , 317.3°E (U.S. Geological Survey, Gazetteer of Planetary Nomenclature, available at <http://planetarynames.wr.usgs.gov>), and lies to

the north of Aromatum Chaos, appears to be present on both the north and south sides of Aromatum Chaos (Figure 2). However, there is no evidence of ejecta on the floor of the depression. This implies that the crater must be older than the termination of subsidence in Aromatum Chaos. The muddy appearance of ejecta around craters such as this strongly suggests that a cryosphere exists underneath the surface [Carr *et al.*, 1977; Squyres *et al.*, 1992]. It is interesting to note that there has been little modification of the surface immediately surrounding the Dia-Cau crater. This may be because of morphological changes caused to the rock by the impact event which made this area more resistant to whatever processes have caused subsidence elsewhere.

[8] The Aromatum Chaos depression consists mainly of a mass of jumbled blocky-chaotic terrain, with the blocks

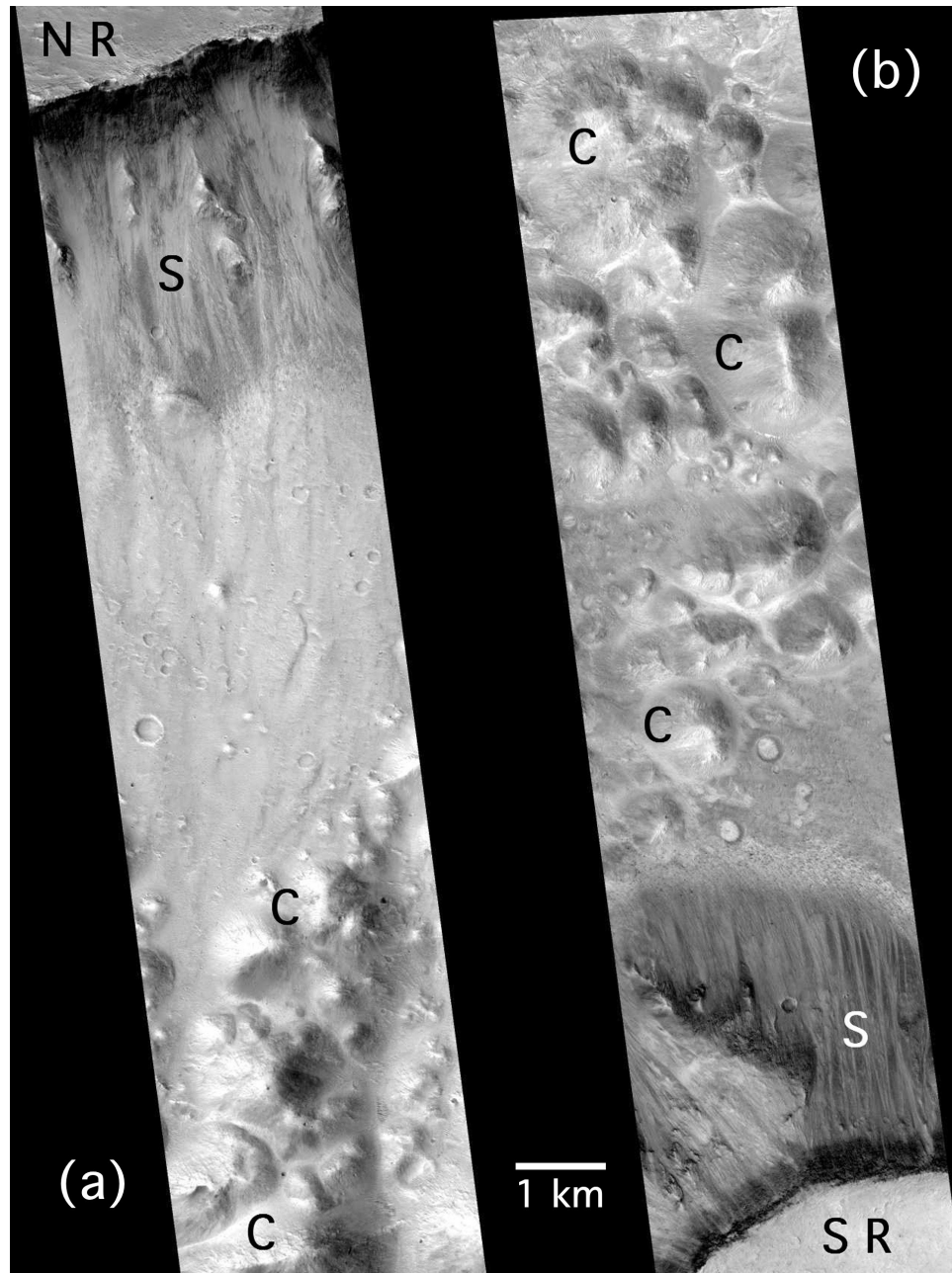


Figure 3. MOC narrow angle images of Aromatum Chaos. North is to the top. Letter C indicates chaotic terrain, and S indicates slopes. (a) Part of the north rim (NR) and adjacent slope and floor. Image width is 3584 m (m0700754). (b) Part of the south rim (SR) and adjacent slope and floor. Image width is 3584 m (m1000810).

generally becoming progressively smaller toward its eastern end (Figure 2). Some of the larger blocks at the western end appear to show evidence of rotational slumping. These larger blocks also appear to be less eroded in that some have flat tops showing a rather angular connection between the flat top and the walls. Similar terrain is found elsewhere on Mars [Sharp *et al.*, 1971], and on Earth this kind of terrain is commonly associated with sliding, slumping, and areas of collapse [Sharp, 1973; Coleman *et al.*, 1978; Carr, 1979; Nummedal and Prior, 1981; Squyres, 1984; Tanaka, 1999; Busche, 2001; Chapman and Tanaka, 2002]. As in many other areas of Mars, some of the chaotic terrain at

Aromatum Chaos has merged with nearby walls (Figures 3a and 3b), as the inward facing escarpment was eroded. This may be in part the result of mass wasting after sapping of volatiles from permeable layers [Masursky *et al.*, 1977; Baker and Kochel, 1979; Schultz *et al.*, 1982; Laity and Malin, 1985; Kochel and Piper, 1986; Chapman and Scott, 1989; Luo *et al.*, 1997].

3. Possible Chaos Formation Mechanisms

[9] The mechanism that has been most commonly proposed for the formation of chaotic terrain on Mars, at

Aromatum Chaos and elsewhere, is the discharge of pressurized water from beneath the cryosphere, which results in the collapse of overlying terrain [Masursky *et al.*, 1977; Baker and Kochel, 1979; Carr, 1979; Theilig and Greeley, 1979; Baker *et al.*, 1991; Lucchitta *et al.*, 1994; Cabrol *et al.*, 1997; Coleman, 2003; Chapman and Tanaka, 2002; Rodriguez *et al.*, 2003; Chapman *et al.*, 2003; Leask *et al.*, 2004; Leask, 2005; Coleman and Dinwiddie, 2005]. This is certainly a plausible suggestion for Aromatum Chaos since it is directly connected to the Ravi Vallis channel system and there is strong evidence from the detailed topography of the region surrounding the Aromatum Chaos depression, especially to the west, for the presence of an extensive subcryosphere aquifer system (Figure 1).

[10] We note that Hoffman [2000, 2001] has suggested that the release of liquid carbon dioxide may have been responsible for the formation of chaotic terrain and eroded channel features on Mars, using Aromatum Chaos and Ravi Vallis as examples. Carbon dioxide is the dominant constituent of the Martian atmosphere and, given the current low average temperatures on and beneath the surface of Mars, Hoffman [2000, 2001] argued that carbon dioxide could theoretically be present beneath the surface in the solid or liquid form, or as a clathrate (a solid solution of CO₂ and water ice). In contrast, Stewart and Nimmo [2001] presented thermodynamic arguments that clathrates may be hard to form by downward diffusion of atmospheric gases into the subsurface, and infer that neither solid CO₂, nor CO₂ clathrate can accumulate in large amounts. However, a so far unexplored possibility is that CO₂ clathrate may form more easily inside volcanoes as a result of the slow upward migration of water and CO₂ degassing from cooling magma bodies [Scott and Wilson, 1999]. Wilson and Head [2002] have pointed out that, even if liquid carbon dioxide were released onto the surface of Mars, its effective travel distance would be limited because of the vastly greater rate (by a factor of about 1000) at which CO₂ evaporates, relative to water, under current Martian atmospheric temperature and pressure conditions. This casts severe doubt on liquid carbon dioxide or CO₂ clathrate being the cause of the outflow channels. Recent authors such as Coleman [2003], Urquart and Gulick [2003], and Rodriguez *et al.* [2003] have also argued against clathrates and for subterranean water as the cause of the chaotic terrain on Mars. In contrast, Hoffman [2000] pointed out that if water had been present on Mars, then carbonates should be present on or near the surface. So far, no significant amounts of carbonate appear to have been detected, but this is no longer surprising in view of the conclusion by Lane *et al.* [2004] that even small amounts of sulphur dioxide will inhibit carbonate formation and lead to sulphate deposition instead.

[11] Max and Clifford [2001] suggested that the sudden decomposition of methane hydrate may have caused thermal and mechanical erosion of the crust. Although the presence of methane hydrate in the Martian subsurface has yet to be confirmed, small amounts of methane have now been detected in the Martian atmosphere [Formisano *et al.*, 2004]. However, both external (cometary impact) and slow internal (alteration of basalts and hydrothermal catalysis of water and carbon dioxide) processes have been discussed as possible sources of the methane [Formisano *et al.*, 2004]. We feel that, at the moment, the involvement

of methane hydrate in chaos formation seems an even less likely scenario than that of CO₂ clathrate.

[12] Pressurized volcanic intrusions, especially dikes, have been widely proposed as a major factor exerting stresses that can lead to disruption of the crust of Mars to allow water release, and possibly causing melting of cryosphere ice to provide at least some of that water [Masursky *et al.*, 1977; Greeley and Spudis, 1981; Mouginiis-Mark *et al.*, 1984; Mars Channel Working Group, 1983; Mouginiis-Mark, 1985; Squyres *et al.*, 1987; Chapman and Scott, 1989; Wilhelms and Baldwin, 1989; Carr, 1990; Mouginiis-Mark, 1990; Cabrol *et al.*, 1997; Tanaka *et al.*, 1998; McKenzie and Nimmo, 1999; Dohm *et al.*, 2001; Max and Clifford, 2001; Chapman and Tanaka, 2002; Rodriguez *et al.*, 2003]. Dikes can also provide heat to prevent water from freezing and, more importantly, can influence the response of crustal aquifers to disruption and lateral water flow [Carr, 1979; Chapman and Tanaka, 1990; Moore *et al.*, 1995; Gilmore and Phillips, 2002].

[13] The role of sills (as sources of heat or stress-induced crustal disruption, or both), has received less attention, though sills have been proposed as factors in producing general features [Squyres *et al.*, 1987; Head and Wilson, 2002; Tanaka *et al.*, 2002] and some specific features [Scott and Wilson, 1999; Wilson and Mouginiis-Mark, 2003; Leask *et al.*, 2004; Leask, 2005] on Mars. A key characteristic of the region studied here is that major collapse is mainly restricted to the structurally controlled Aromatum Chaos depression. We contend that the simplest explanation is the intrusion of a sill beneath the area now defined by the chaotic terrain. Intrusion of the sill and its feeder dike(s) applied stresses to the cryosphere rocks in addition to enhancing the local heat flow at shallow depth and melting cryosphere ice. The combination of these factors caused fracturing of the cryosphere and vertical movements within it, thus allowing pressurized water from an underlying aquifer to rise vertically through the pathways created before flowing laterally out of the depression, causing erosion at all stages.

4. Implications of the Geometry of Aromatum Chaos

[14] Measurements on THEMIS images show that the main Aromatum Chaos depression (see Figure 2) is approximately 91.5 km long in the southwest-northeast direction and on average 30 km wide at right angles to this direction. The geometry of the interior of the depression was investigated quantitatively as follows. All MOLA profiles that crossed the uppermost parts of raised floor blocks were examined, and 30 were found that between them crossed the highest parts of 20 blocks. The absolute positions of the tops of the blocks relative to the MOLA datum were noted, and the estimated depths of the tops of the blocks below the position of the precollapse surface, extrapolated linearly between the two rims of the depression, were measured. A smooth curve was fitted through each profile to pass through all the local topographic minima, in an attempt to locate the greatest potential extent of collapse or erosion. In the example shown in Figure 4, the smooth curve that best fits the minima in this case is a fifth-order polynomial. The heights of the tops of the blocks were measured both above

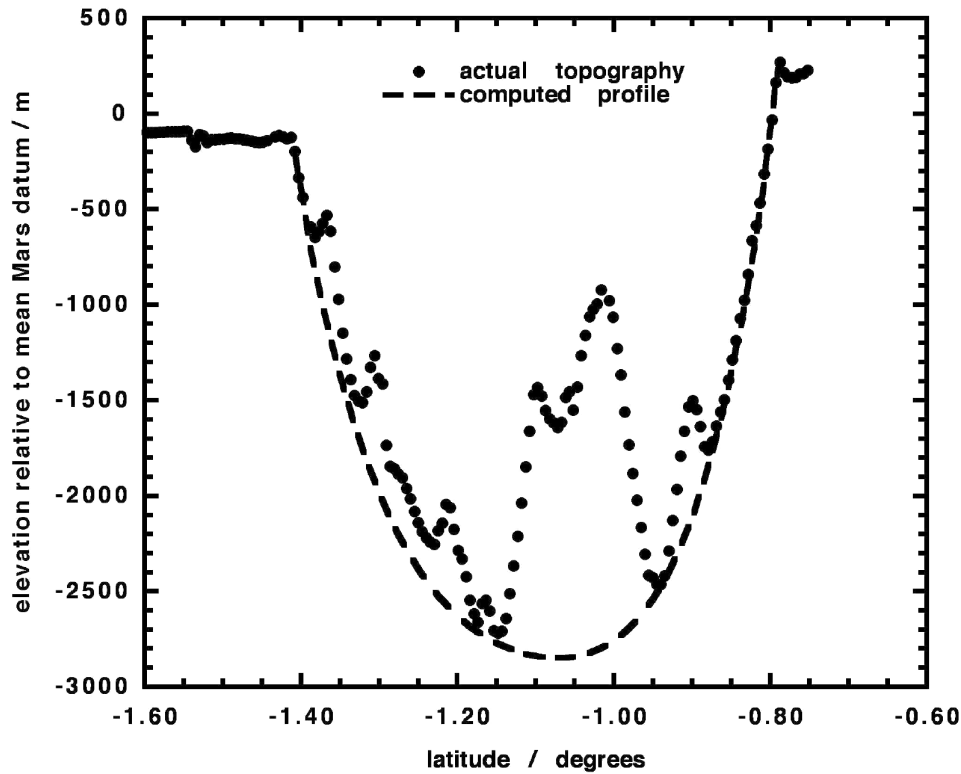


Figure 4. North-south profile of Aromatum Chaos showing actual topography of the floor surface taken from MOLA track 11982 and a computed parabolic profile of the implied underlying depth of the floor. Each degree of latitude is ~ 60 km.

the local floor (the observed vertical extent of the block), and above the possible floor position as determined from the fitted curve (the extrapolated maximum vertical extent of the block). Table 1 shows all of the measurements.

[15] The tops of the blocks lie between 1010 m and 2360 m below the rim of Aromatum Chaos, and between

~ 470 m and ~ 1950 m above the inferred maximum floor location (Table 1). Figure 5 shows the variation as a function of longitude of the absolute positions of the tops of the blocks in Figure 5a, the depths below the inferred precollapse surface in Figure 5b, the observed vertical extents of the blocks in Figure 5c and the possible maxi-

Table 1. Measurements on Terrain Blocks on the Floor of Aromatum Chaos^a

MOLA Track Number	Longitude, °E	Latitude, deg	Absolute Elevation Relative to MOLA Datum, m	Depth Below Precollapse Surface, m	Observed Height Above Local Floor, m	Extrapolated Height Above Inferred Floor, m
18053	316.497	-0.986	-1115	1195	745	905
19569	316.507	-1.196	-1100	1140	1035	1060
11333	316.522	-1.012	-1470	1555	1200	960
11774	316.561	-1.224	-1445	1415	1045	1260
11774	316.567	-1.265	-1445	1410	885	1100
11982	316.588	-1.306	-1265	1245	635	785
11982	316.626	-1.016	-920	1020	1550	1940
14002	316.639	-1.029	-960	1085	1350	1950
20107	316.667	-1.245	-1285	1275	1250	1680
16259	316.716	-1.265	-1970	1995	900	995
18787	316.730	-1.270	-2165	2080	875	935
14332	316.732	-1.205	-2215	1845	1195	1365
14210	316.749	-1.366	-1075	1095	1425	1480
13879	316.761	-1.362	-1110	1120	1400	1635
19765	316.779	-1.346	-980	1010	1580	1785
19765	316.795	-1.224	-1840	1950	1175	1310
14650	316.814	-1.338	-1785	2015	595	575
19960	317.012	-1.069	-1730	2035	1005	1300
12814	317.097	-1.025	-1900	2360	735	800
17147	317.295	-1.020	-1680	1950	455	470

^aValues are rounded to ± 5 m to reflect accuracy of MOLA instrument.

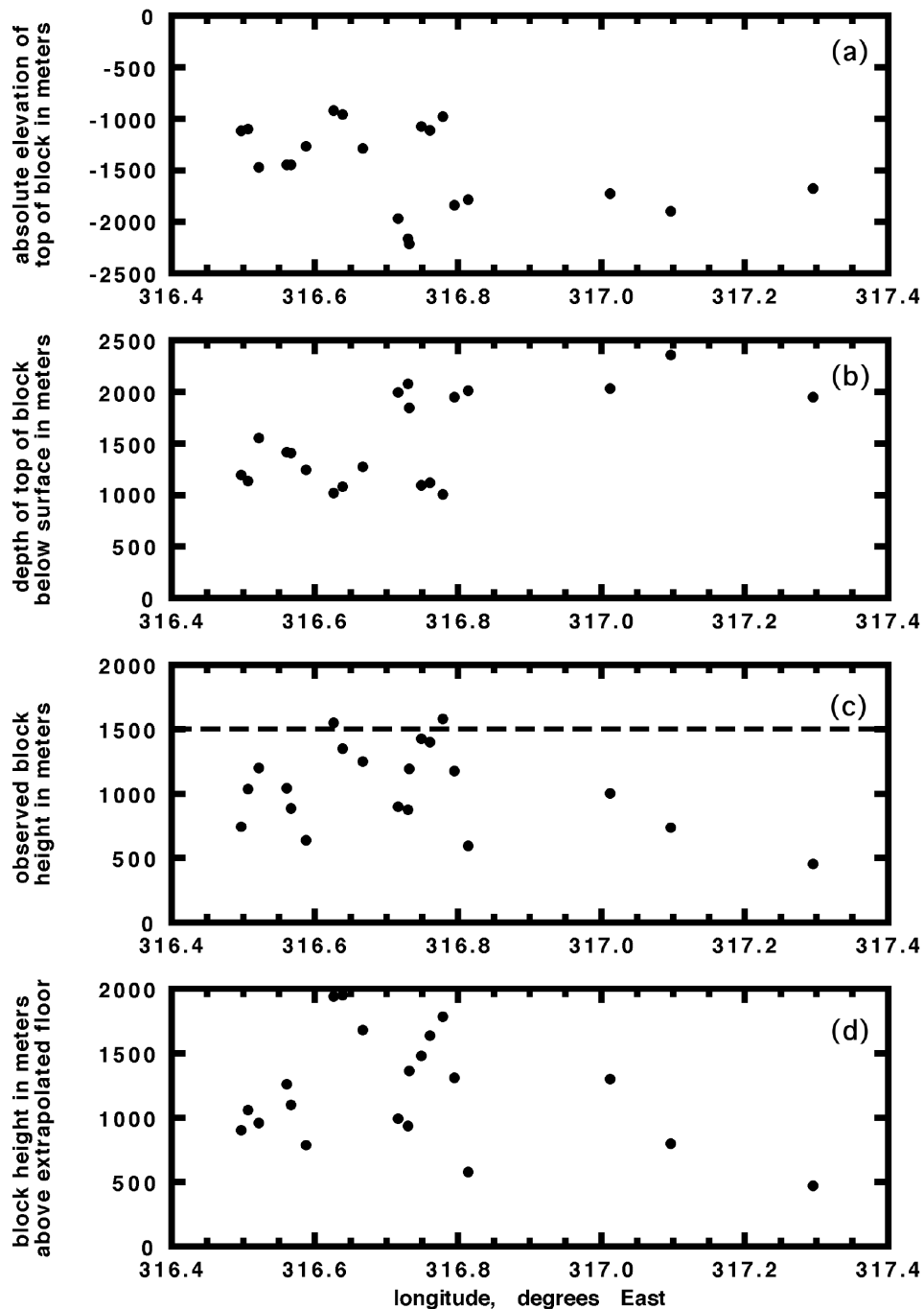


Figure 5. Topographic properties of blocks on floor of Aromatum Chaos for which MOLA profiles cross tops of blocks: (a) absolute elevation relative to Mars MOLA datum of tops of blocks, (b) depths of tops of blocks below extrapolated local surface, (c) observed block heights above local floor of depression, and (d) block heights above extrapolated floor.

imum extents of the blocks in Figure 5d. These variations with longitude (and also the equivalent plots as a function of latitude) were examined for signs of trends that might imply some spatially varying structural control of the block subsidence process, but none was found.

[16] The maximum extrapolated depth of the depression below the rim was extracted from each of the MOLA profiles (the minimum of each of the smooth curves like that shown in Figure 4), and the values were plotted as a

function of longitude (Figure 6) with a smooth curve giving the envelope of all the depths. This shows that the maximum depth of the floor is about 3.45 km below the rim level. The volume of material removed from Aromatum Chaos was estimated as follows. The area was obtained as the product of the lengths mentioned above, $91.5 \text{ km} \times 30 \text{ km} = 2745 \text{ km}^2$. The mean depth of the western two thirds of the depression, 1.64 km, was estimated by finding the mean depth below the extrapolated precollapse ground

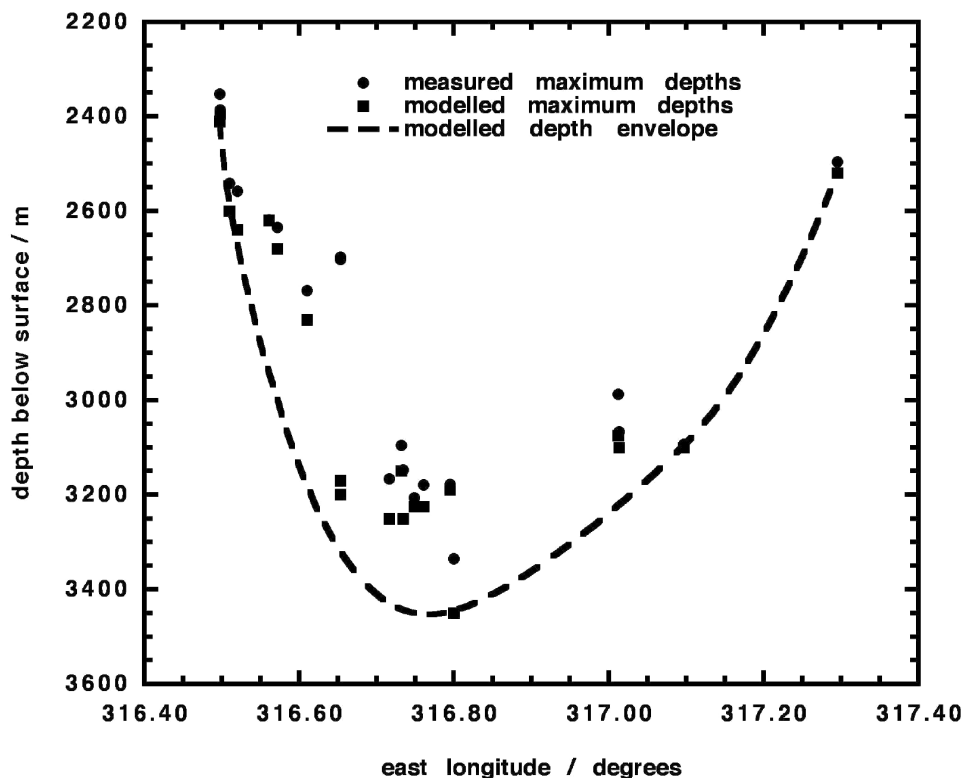


Figure 6. Composite east-west profile of Aromatum Chaos showing measured deepest points on floor surface, taken from MOLA data, and a modeled depth envelope for the floor. Deepest measured point is ~ 3.45 km below Mars datum. Each degree of longitude is ~ 60 km.

surface along all of the 30 MOLA profiles crossing the depression. The remaining eastern one third of the area has much less relief than the western part, and so its depth was judged by eye from the MOLA topographic contours to be $\sim 1.20 \pm 0.05$ km. The overall average depth is thus $(2/3) \times 1.64$ km + $(1/3) \times 1.20$ km = 1.49 km, making the total volume missing from Aromatum Chaos 2745 km² \times 1.49 km = 4090 km³.

[17] It is clear that this missing volume cannot consist solely of ice that has melted and either evaporated or seeped away, allowing compaction of the pore space. *Hanna and Phillips* [2003, 2005] and *Clifford* [1993] give estimates of the porosity of the outer 10 km of the Martian lithosphere (see Figure 7). Essentially, the porosity at depths shallower than ~ 1 km is 15 to 20% and at all greater depths that are relevant it is $\sim 4 \pm 1$ %. If all of this pore space were filled with ice, and all of the pore space were completely compacted by removal of the ice (neither of which condition is likely to be fully reached), then desiccation of the upper 1 km with 20% porosity would yield 0.2 km of collapse, and desiccation of a further 36 km vertical extent at 4% porosity would be needed to explain the remaining 1.64 km – 0.2 km = 1.44 km collapse of the deepest part of the depression. The cryosphere could not possibly have the implied depth of ~ 37 km; this can be demonstrated as follows. Using *McGovern et al.*'s [2002] estimate of the present-day heat flux of 20×10^{-3} W m⁻², and taking the thermal conductivity of the cryosphere to be ~ 2.5 W m⁻¹ K⁻¹ (the values for both silicate rock and ice are close to this value at the temperatures involved), the temperature gradient

is 8 K km⁻¹. If the mean surface temperature at the location of Aromatum Chaos near the equator is taken as ~ 230 K it follows that the base of the cryosphere is at a depth of $(273 \text{ K} - 230 \text{ K})/8 \text{ K km}^{-1} = \sim 5.4$ km. Thus the absolute maximum extent of collapse that could be due to ice removal is about 0.2×1 km + 0.04×4.4 km = 0.376 km. It follows that most (nominally $\sim 77\%$) of the material removed was crustal rock. If we took account of the fact that the geothermal gradient on Mars may have been higher at the time of formation of Aromatum Chaos, say 30×10^{-3} W m⁻² [*McGovern et al.*, 2002], and the thermal conductivity of the cryosphere may have been smaller than the value used above, say ~ 2 W m⁻¹ K⁻¹ to allow for the effects of pore space unoccupied by ice, the geothermal gradient would have been ~ 15 K km⁻¹, the cryosphere thickness ~ 2.9 km, the extent of collapse about 0.2×1 km + 0.04×1.9 km = 0.276 km, and the proportional of material removed that was crustal rock $\sim 83\%$.

[18] It should be noted that the estimates given in the previous paragraph, and many that follow later in this paper, depend strongly, and in a nonlinear way, on the porosity and ice content profiles assumed for the crust of Mars. Thus, even a 50% error in the 20% porosity value assumed for the outer 1 km of crust would have led to only a 7.5% error in the implied (improbable) 37 km cryosphere thickness if the 4% average porosity of the deeper layers were correct. However, our suggested 25% error in that deeper porosity value would have produced up to a $\sim 30\%$ error in the cryosphere thickness estimate. Throughout the paper we provide details of all of the steps in the calculations so that

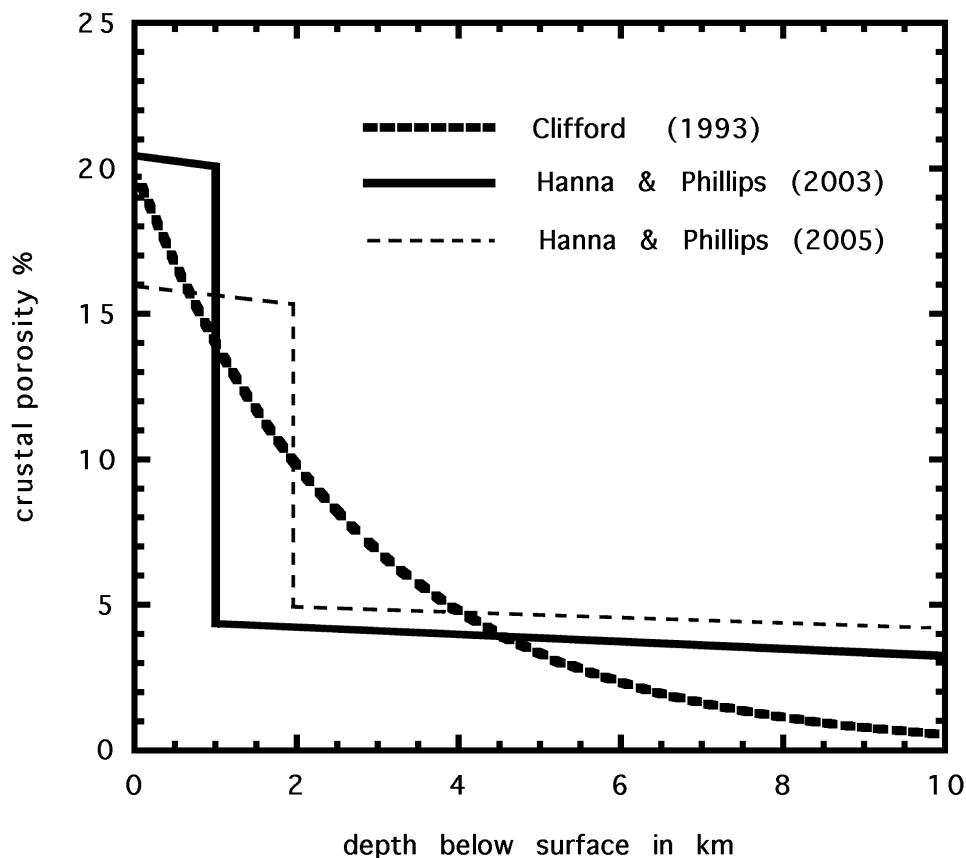


Figure 7. Comparison between models of variation of crustal porosity with depth below surface of Mars by *Clifford* [1993] and *Hanna and Phillips* [2003, 2005].

the consequences of future improvements in knowledge of the crustal structure of Mars can easily be incorporated.

[19] Some of the large positive terrain features on the floor of the Aromatum Chaos have flat tops, and a few appear to have rotated to some extent as they have subsided as coherent blocks of rock. We infer that these blocks are pieces of cryosphere that did not thaw as a result of the intrusion, and hence subsided largely intact; thus their vertical sizes set a limit to the shallowness of the top of the zone of hydrothermal circulation and ice melting above the proposed sill. As shown in Figure 5c, the subsided blocks are typically up to ~ 1.5 km in vertical extent. We infer that, at the locations of the blocks, ice has only been removed from the cryosphere at depths greater than ~ 1.5 km, whereas both ice and rock have been removed from the areas between these blocks. It was determined, by thresholding and pixel counting in a mosaic of THEMIS images of the Aromatum Chaos, that subsided blocks occupy $\sim 17\%$ of the floor area, with no significant difference between the western two thirds of the depression and the eastern one third. Weighting the porosity for the vertical and horizontal proportions that have 20% and 4% porosity down to the base of the cryosphere at 5.4 km depth, we find that the average porosity of the material removed from the depression would have been 6.45%. If the pore space had been filled with ice, the equivalent total ice thickness would then have been 105 m in the western two thirds of the depression and 75 m in the eastern one third, making the

total ice volume ~ 260 km³; the equivalent dense rock thicknesses would have been 1535 m in the western part and 1125 m in the eastern part, making the total rock volume ~ 3840 km³. The errors in these ice and rock volumes due to permuting porosities between 15 and 20% in the shallow part of the cryosphere and between 3 and 5% in the deeper cryosphere are $\sim 20\%$.

5. Removal of Material From Aromatum Chaos

[20] We now address the elutriation of material from the Aromatum Chaos depression by the water rising from an underlying aquifer. In a companion paper [*Leask et al.*, 2006] we show that, after some decline in the discharge from an early high value, water was flowing out of the eastern end of Aromatum Chaos into Ravi Vallis, for much of the duration of the water release, with a speed of ~ 10 m s⁻¹ and a depth of ~ 100 m, the total volume flux being $\sim 1 \times 10^7$ m³ s⁻¹. This water must have risen through a series of fractures that extended through the sill and overlying cryosphere to the surface. The horizontal sizes of the larger subsided and slumped blocks of crust resting on the floor of the chaos (Figure 2) suggest that in its western part, these fractures were separated by distances of order 3 km. Given the thickness of the cryosphere, the fractures must have initially extended vertically for more than 5 km, though later, after some material had been removed by water flow, their vertical extents would have been closer to 4 km. If these fractures were held open

Table 2. Values for the Upward Speed That Water Must Have to Transport Clasts Toward the Surface Through the Fractures Beneath Aromatum Chaos for a Range of Sizes of Clasts With Density 2500 kg m^{-3}

Clast Diameter	Water Speed, m s^{-1}
1 μm	2.1×10^{-7}
10 μm	2.1×10^{-5}
100 μm	2.1×10^{-3}
1 mm	4.3×10^{-2}
1 cm	0.14
10 cm	0.43
1 m	1.36

elastically, their width to length ratios would have been of order P/μ , where P is the excess pressure driving the water up the fracture and μ is the shear modulus of the cryosphere material, $\sim 5 \text{ GPa}$. Treatments of water rise up fractures elsewhere on Mars [Head *et al.*, 2003] suggest that P is at least $\sim 10 \text{ MPa}$; this implies a width to length ratio of 0.002, and for a vertical extent of 4 km this produces a width of 8 m. For comparison, in analyzing the water release fractures along the Cerberus Fossae feeding the Athabasca Valles outflow channels, Head *et al.* [2003] found fracture widths of ~ 2 to 3 m. A rectangular grid of 8 m wide fractures with 3 km spacing over the $40 \times 30 \text{ km}$ western end of the chaos (Figure 2) would have a surface area of about $6.3 \times 10^6 \text{ m}^2$; the $40 \times 30 \text{ km}$ region represents about 44% of the entire area of the chaos and so it is reasonable that it delivered 44% of the $\sim 1 \times 10^7 \text{ m}^3 \text{ s}^{-1}$ total water flux, i.e., $\sim 4.4 \times 10^6 \text{ m}^3 \text{ s}^{-1}$. This flux, rising through the $6.3 \times 10^6 \text{ m}^2$ area of fractures, would imply an average water rise speed, U , of 0.7 m s^{-1} . If the fractures had been narrower, the rise speed would have been greater; thus, if the fracture widths had been the 2 to 3 m found at Athabasca, the typical water rise speed would have been ~ 2 to $\sim 3 \text{ m s}^{-1}$.

[21] We can find the sizes of rock fragments that this water speed would just support by equating the effective weight of a (for convenience spherical) clast of diameter D and density ρ to the drag force acting on it. The weight is $[(4/3) \pi (D/2)^3 (\rho - \sigma) g]$ where σ is the water density and g is the acceleration due to gravity, and the drag force is $[6 \pi \eta (D/2) U]$ if the water flow around the clast is laminar and $[(1/2) \sigma C_D \pi (D/2)^2 U^2]$ if it is turbulent, where η is the water viscosity and C_D is a dimensionless drag coefficient of order unity. The decision as to which is the correct drag force expression is decided on the basis of self-consistency with the implied clast Reynolds number $[(D U \sigma)/\eta]$, which must be less than ~ 2000 for laminar water flow. Table 2 shows the results of these calculations for a wide range of diameters of clasts with a density of 2500 kg m^{-3} . The conservative water rise speed of 0.7 m s^{-1} would have transported upward all clasts smaller than $\sim 25 \text{ cm}$, and the alternative ~ 2 to $\sim 3 \text{ m s}^{-1}$ water speed would have carried clasts more than 1 meter in size. As solid material reached shallow levels, it would encounter the more nearly horizontal flow of water moving toward the Ravi Vallis outlet. The horizontal water speed would have varied roughly linearly with position within Aromatum Chaos, and with a value of $\sim 10 \text{ m s}^{-1}$ at the outlet and a west-east chaos extent of $\sim 90 \text{ km}$ it would have had a value of $\sim 1 \text{ m s}^{-1}$ at a distance of $\sim 10 \text{ km}$ from the western end. Thus we expect that

transport and removal of all but the coarsest material into which the cryosphere might have disaggregated would have been easy except within $\sim 10 \text{ km}$ of the western end of the chaos, a region largely occupied by slump blocks (Figure 2) and from which, indeed, less material has been removed than elsewhere (Figure 6).

6. Aquifer Water Volume and Implied Aquifer Area

[22] The water that flowed out of Aromatum Chaos and through the associated channel system of Ravi Vallis must have carried all of the rock removed from the Chaos depression and also all of the rock eroded to form the channel system (we assume that the ice component of the cryosphere was melted during the erosion process). In a companion paper [Leask *et al.*, 2006] we analyze the detailed processes involved in the formation of Ravi Vallis and describe there the derivation of the total volume eroded to form the valley system and the estimation of the proportion of eroded material that is ice. The volumes obtained are 3350 km^3 of rock and 840 km^3 of ice; the errors in these volumes, $\sim 20\%$, are dependent on the porosity profile assumed for the cryosphere in the same way as the volumes found in this paper. Thus combining these volumes with those found in section 4 for the material removed from the depression, the total volumes of material excavated from the entire Aromatum-Ravi system are $\sim 7190 \text{ km}^3$ of rock and $\sim 1100 \text{ km}^3$ of ice.

[23] Estimates of the ability of water flowing in channels to transport sediment suggest that an upper limit is $\sim 40\%$ by volume sediment load [Komar, 1980; Smith, 1986; Costa, 1988]. We can therefore use the volume of rock missing from the Aromatum Chaos depression to estimate the minimum volume of water, V_o , that must have overflowed from the depression to carry the rock away. If 40% by volume of the total flood is the 7190 km^3 volume of rock, the remaining 60% is water, so that V_o is $10,785 \text{ km}^3$. For completeness we give total implied water volumes for carrying capacities of 40, 30, 20 and 10% in Table 3. We also include for each case the corresponding volume of water, V_e , extracted from the underlying aquifer. This is evaluated by adding to V_o the volume of water V_r that would have been left as a residual (inevitably ice covered) lake inside the Aromatum Chaos depression at the end of the water release event, and then subtracting from that total

Table 3. Various Assumptions About the Sediment Carrying Capacity of Flowing Water, S , and Values for the Volume of Water, V_o , Required to Carry Away the Rock Missing From Aromatum Chaos and the Corresponding Volume of Water, V_e , That Must Have Been Extracted From the Underlying Aquifer^a

S , vol %	V_o , km^3	V_e , km^3	A_a , km^2
40	10,785	10,565	70,430
30	16,780	16,560	110,400
20	28,760	28,540	190,270
10	64,710	64,490	429,930

^aValues of the corresponding aquifer surface areas, A_a , are also given on the assumption that the aquifer has a 5 km vertical extent and a porosity of 3%. See text for details.

the volume of water V_m produced by the melting of the cryosphere ice. We have already seen that the ice volume was $\sim 1100 \text{ km}^3$ and so, adjusting for the densities of water (1000 kg m^{-3} just above the melting point) and ice ($\sim 926 \text{ kg m}^{-3}$ at the $\sim 210 \text{ K}$ average temperature relevant to the shallow cryosphere), V_m is $\sim 1019 \text{ km}^3$. V_r can be evaluated by noting that the floor of the depression at the point where Aromatum Chaos joins Ravi Vallis is at a depth of $\sim 1.2 \text{ km}$, making the average depth of the lake about $1.49 - 1.2 = 0.29 \text{ km}$ and its volume $0.29 \text{ km} \times 2760 \text{ km}^2 = 800 \text{ km}^3$.

[24] Estimates of the volume of aquifer water released can be used to deduce corresponding values of the implied surface area of the aquifer if we know its vertical extent and water capacity. Figure 7 suggests that at depths greater than $\sim 5 \text{ km}$ a representative average porosity is $\sim 3\%$. The location of the upper limit of the aquifer is the base of the cryosphere at 5.4 km depth, and so the aquifer would have had a vertical extent of $\sim 10 \text{ km} - \sim 5.4 \text{ km} = \sim 5 \text{ km}$. With an average 3% porosity, the equivalent thickness of water in the aquifer would be $0.03 \times 5 \text{ km} = 0.15 \text{ km}$. The required aquifer surface area implied by each of the water volumes in Table 3 can be obtained by dividing the water volume by this value. The area corresponding to the $10,565 \text{ km}^3$ water volume implied by a 40% debris load in the flood is $10,565 \text{ km}^3 / 0.15 \text{ km} = \sim 70,430 \text{ km}^2$. The values corresponding to 30% , 20% and 10% debris loads are $\sim 110,400$, $\sim 190,270$ and $\sim 429,930 \text{ km}^2$, respectively. These areas are ~ 26 , ~ 40 , ~ 69 and ~ 156 times greater, respectively, than the 2745 km^2 area of the Aromatum Chaos depression. The somewhat depressed triangular region to the west of Aromatum Chaos shown in Figure 1 has an area of $\sim 37,000 \text{ km}^2$. This is about half the aquifer area required to explain a 40% sediment load in the water escaping through the depression and an even smaller fraction of the areas corresponding to the larger water estimates. Thus, although the proximity of this area of incipient collapse to Aromatum Chaos makes it an attractive candidate for the water source area, it is clear that a much larger reservoir would have been needed as the water source, thus providing quantitative support for the suggestion that Gangis Chasma was the main water source for both the Aromatum-Ravi system and Shalbatana Vallis [e.g., Nelson and Greeley, 1999; Coleman, 2002, 2003, 2004; Rodriguez et al., 2003].

[25] It is worth noting that the shallowest part of the floor of Shalbatana Vallis, with an absolute elevation of -2.7 km at 2°N , 316.5°E , is deeper than the lip joining Aromatum Chaos to Ravi Vallis at -1.2 km , but is shallower than the deepest part of Aromatum Chaos at -3.45 km . This suggests that, if the water releases at Shalbatana Vallis and Ravi Vallis were part of the same thermal episode, then even though water had ceased to flow into Ravi Vallis it could still have been supplied to Shalbatana Vallis while maintaining a lake within Aromatum Chaos [Leask, 2005].

7. Sill Thickness and Depth of Intrusion

[26] The problem of heat transfer from sill intrusions into the surrounding cryosphere on Mars has been addressed by Squyres et al. [1987]. Conditions above and below the sill differ somewhat in that convection of water occurs above the sill, but not below, where heat transfer is essentially by conduction alone. Squyres et al. [1987] calculated that for a

sill thickness of 10 m at a depth of 100 m in a cryosphere containing 25% ice, the thickness of the layer containing water exceeds the thickness of the sill by a factor of ~ 2 to 4 . When the burial depth is less than a value about equal to the sill thickness, a significant amount of heat is lost to the surface, reducing the extent of water melting, but sill injections at sufficient depth below the surface of an ice-rich cryosphere can form net depressions after lateral drainage of water, or water loss to the atmosphere.

[27] The case considered here is different in that we are assuming a much smaller ($\sim 4\%$ as against 25%) ice content in the cryosphere than did Squyres et al. [1987]. This makes it difficult to extrapolate their results to our case, and so we implemented an analytical model of sill cooling based on equation (16) of Carslaw and Jaeger [1947, chapter 2, section 20 [v]]. The model assumes that a layer of hot material (the sill) is intruded instantaneously into an infinite region of colder material at a uniform temperature and evaluates the subsequent temperature distribution in both materials as a function of depth and time. Geometric constraints (up to $\sim 1.5 \text{ km}$ vertical sizes of subsided blocks of unheated crust and $\sim 5.4 \text{ km}$ thickness of cryosphere) imply the center of the sill to be located between ~ 2 and $\sim 5 \text{ km}$ below the surface, and using our earlier estimate of the geothermal gradient this implies a host temperature between ~ 230 and $\sim 270 \text{ K}$; we use 240 K and 250 K in the following illustration. We find that the sill is sufficiently deep that the finite depth below the planetary surface does not greatly perturb the model solutions. The Carslaw and Jaeger model requires constant values for the thermal properties of the sill magma and the host material, whereas in reality they are temperature dependent. For the sill magma we use an average specific heat over the cooling interval of $900 \text{ J kg}^{-1} \text{ K}^{-1}$. The dominance of the rock component in the host material means that we can approximate the bulk values of density and thermal conductivity by appropriately proportion-weighted averages. We allow for the latent heat of melting of ice (and, if it occurs, vaporization of water) by computing an effective specific heat and hence thermal diffusivity for the host material at all temperatures between the initial ambient and the sill temperature (taken as 1450 K assuming a basaltic magma). The effective specific heat is obtained by finding the total enthalpy (the total of the sensible and latent heats) per unit mass corresponding to a given temperature rise and dividing it by the temperature rise. The ratio of the effective thermal diffusivity of the H_2O -rock mixture to the thermal diffusivity of the rock component alone ($\sim 7 \times 10^{-7} \text{ m}^2 \text{ s}^{-1}$) ranges from 1.0 to 0.64 ; the average over all relevant temperatures is 0.76 , leading to a bulk thermal diffusivity of $(0.76 \times 7 \times 10^{-7} =) 5.3 \times 10^{-7} \text{ m}^2 \text{ s}^{-1}$. We estimate that these various approximations introduce at most a 20% error relative to a completely detailed numerical treatment.

[28] The temperature of the sill magma decreases as a function of time after sill emplacement and heat diffuses into the host rocks. The temperature at a given distance above and below the sill margin first increases to some maximum value and then decreases again. Figure 8 shows the total vertical extent of the zone above and below the sill within which ice is melted as a function of time for a 30 m thick sill emplaced at depths where the ambient temperature is 240 K and 250 K . The distances are given as the ratio of

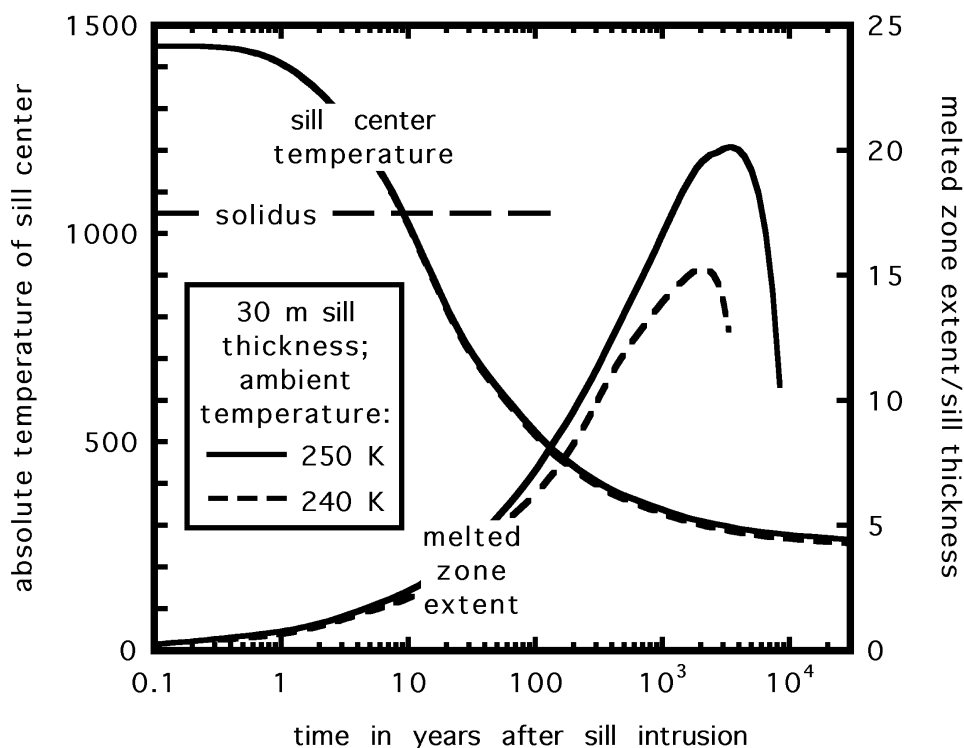


Figure 8. Calculated sill center temperature (left axis) and ratio of extent of melted zone to sill thickness (right axis) as a function of time after sill emplacement for a 30 m thick sill. Curves are shown for ambient cryosphere temperatures of 240 K and 250 K.

the vertical extent of the zone to the sill thickness because this ratio is independent of sill thickness itself. Also shown in Figure 8 is the temperature of the center of the sill when a given zone size is attained. Both the time after sill intrusion at which a given melted zone ratio is reached and the time at which a given sill temperature is reached are found to be directly proportional to the square of the sill thickness. Thus, for a 300 m thick sill, ten times thicker than that shown, the times on the abscissa of Figure 8 would increase by a factor of 100 but the shapes of the curves would be unchanged.

[29] The horizontal dashed line in Figure 8 indicates the solidus temperature, ~ 1060 K, of the basaltic magma in the sill. Our model of the initiation of water release from a trapped aquifer beneath Aromatum Chaos calls for disaggregation of the cryosphere due to ice melting, and must also require fracturing of the sill to allow water to pass through it. We assume that any large-scale disturbance of the sill will be self-healing as long as it contains some molten magma, but that the sill will become susceptible to brittle failure after all of it has cooled well below the solidus. Thus if the sill were 30 m thick, the case shown, we might expect some fracturing of the sill by ~ 50 years after the volcanic event emplacing it, at which time a vertical extent of about 5 sill thicknesses, i.e., ~ 150 m, of cryosphere will have been thawed. Complete drainage of water and compaction of the 4% pore space, assuming that this were possible, would have produced ~ 6 m of subsidence to counteract the 30 m of uplift due to the intrusion. If sill fracture had been delayed until ~ 200 years after intrusion, the thawed zone would have been 300 m in extent and the

subsidence would have been 12 m, still less than one half of the uplift. If the sill had been 100 m thick, the corresponding short-term events would have occurred ~ 550 years after the intrusion, by which time ~ 500 m of cryosphere would have thawed, yielding a maximum of 20 m of subsidence after the ~ 100 m of uplift; delayed activity would have occurred 2200 years after the intrusion with 40 m of subsidence countering the 100 m of uplift. An even thicker sill would cause even more extensive melting, but if the sill thickness had been several hundred meters its intrusion should have produced enough uplift, even after water drainage, in the vicinity of the rim of Aromatum Chaos to be detectable in the MOLA data, and our careful examination of the highest-resolution MOLA contours shows no sign of systematic uplift on this scale. We conclude that the sill was probably no more than ~ 100 m to at most 200 m thick.

[30] Fracturing of the sill and adjacent cryosphere may have been aided by pressure changes in the water produced by ice melting. The critical pressure for water, ~ 22.1 MPa, is equal to the lithostatic pressure at a depth of ~ 2.4 km in the Martian cryosphere, and given the constraints on sill intrusion depth, ~ 2 to ~ 5 km, the water close to the sill would have been in its super-critical fluid state for a considerable length of time after ice melting. Attempts to assess the possible pressure increase as this fluid was heated are limited partly by the availability of thermodynamic data for H_2O at very high pressures and partly by our lack of knowledge about the cryosphere; if the cryosphere pore space was not completely filled by ice then some of the fluid volume changes could have been accommodated by

invasion of available space rather than pressure increases. As a conservative example, for a 100 m thick sill intruded at 5 km depth, if ice formed 4% of the cryosphere volume but there was an extra 4% of vacant space available, data tabulated by *Department of Scientific and Industrial Research* [1964] show that the fluid pressure would have exceeded the lithostatic pressure by ~ 10 MPa (greater than the likely strength of the cryosphere and almost certainly initiating fractures in it) when the temperature reached ~ 700 K. The model calculations show that this temperature was exceeded in a zone 15 m deep below the sill for ~ 130 years after its center cooled to the solidus. More complete ice filling of the pore space would have led to similar pressure increases over a greater range of depths.

[31] At what depth was the sill emplaced? The minimal requirement is that it lay within the cryosphere to have significant thermal effects. Further, its base must have been far enough above the base of the cryosphere so that some movement could take place in the cryosphere below the sill to allow gaps to form within the cooling magma sheet so that water could be forced up through the sill. If, as assumed earlier, the slumped and sometimes rotated blocks on the floor of the Aromatum Chaos depression represent pieces of cryosphere that subsided largely intact, the differences in level between the tops of nearby blocks can be taken as a guide to the vertical displacements within the thawed zone beneath the sill, typically up to 300 m. Figure 8 shows that a thawed zone 300 m thick beneath the sill would be produced if the sill were 120 m thick, which is within the range implied by the uplift constraints. If the thawed zone above the sill were also 300 m thick, then the need to keep the outer 1.5 km of the crust frozen, as implied by the presence of the intact blocks on the floor of the chaos, would place the top of the sill deeper than ~ 1.8 km.

8. Discussion

[32] There are inevitably a number of uncertainties in the measurements and calculations presented here. Errors in elevation measurements derived directly from MOLA topography and from interpolating between MOLA orbits are small compared with uncertainties in the porosity, and hence ice content and thermal conductivity, of the cryosphere, and in the geothermal heat flux at the time of formation of Aromatum Chaos. In particular, we note that increasing the heat flux and reducing the thermal conductivity of the cryosphere from the values chosen here to values arguably equally plausible for the Hesperian to Amazonian period could reduce the cryosphere thickness from 5.4 km to 2.9 km. However, with this value it would still be possible to fit the postulated sill and associated zones of collapse and deformation into the vertical space available.

9. Summary

[33] 1. Our morphological examination of the Aromatum Chaos depression, the Ravi Vallis outflow channel to which it is connected, and the region surrounding it in Xanthe Terra lead us to support earlier suggestions in the literature that Aromatum Chaos was the site of crustal disruption, water release from an underlying pressurized aquifer, elutriation of crustal rock by the rising water, and concomitant

crustal collapse. On the basis of the shape of its boundaries, we specifically propose that the Aromatum Chaos depression delineates the area occupied by a dike-bounded sill that intruded the cryosphere and caused thermal and mechanical disruption. Figure 9 summarizes the five main stages in the development of the depression. In an attempt to test this proposal we have made a number of quantitative measurements on the geometry of the Aromatum Chaos depression and the raised blocks of crustal material present on its floor.

[34] 2. The tops of the raised blocks of terrain on the floor of the depression lie between 1010 m and 2360 m below the inferred location of the surface before the depression formed, and between ~ 470 m and ~ 1950 m above the extrapolated maximum depth of the floor (Table 1). We infer that the blocks represent parts of the shallow cryosphere that have subsided largely intact when ice in the deeper cryosphere melted and allowed rising water to flush fractured rock out of the depression into Ravi Vallis. There appears to be no structural control of the distances that the blocks have subsided, but their maximum vertical extents imply that melting was confined to depths greater than ~ 1.5 km.

[35] 3. The maximum depth of the Aromatum Chaos depression was measured to be 3.45 km and its mean depth is 1.49 km; its surface area is about 2760 km². The volume of material missing from the crust is ~ 4090 km³ and, based on the crustal porosity models of *Hanna and Philips* [2003, 2005] and *Clifford* [1993], we estimate that this is composed of 260 km³ of ice and 3840 km³ of rock.

[36] 4. Using an analytical model of heat release from an intrusion that closely approximates the conditions in the Martian cryosphere, we find the thickness of the sill required to produce the effects seen at Aromatum Chaos to be a little greater than 100 m. The location of the sill is constrained by the vertical extents of the blocks of terrain on the floor of Aromatum Chaos and the need for melting of ice below the sill to allow for the vertical movements associated with the fractures through which water rose from the underlying aquifer. Taken together these requirements imply that the center of the sill is located at a depth between ~ 2 and ~ 5 km. The water rise speed through the fractures is estimated to have been at least 0.7 m s⁻¹, making it capable of lifting up to 0.25 m sized clasts (Table 2) to shallow levels, where they would be entrained into the lateral water flow toward Ravi Vallis.

[37] 5. The minimum volume of water that would have had to rise through the Aromatum Chaos depression in order to transport the missing rock away as sediment in the catastrophic flood that traveled down Ravi Vallis is a function of the sediment-bearing capacity of the water. For sediment volume loads of 40, 30, 20 and 10% the implied required water volumes are estimated to be $\sim 10,600$, $\sim 16,600$, $\sim 28,500$ and $\sim 64,500$ km³, respectively (Table 3). The water passing through Aromatum Chaos could have lifted and carried away all silicate materials with clast sizes smaller than ~ 25 cm.

[38] 6. On the assumption that the water which welled up through Aromatum Chaos was derived from an aquifer ~ 5 km in vertical thickness with a porosity of $\sim 3\%$, we derive the implied areas of the aquifer system required to supply the flood (Table 3). For a 40% sediment load the area is $\sim 70,400$ km², nearly double the $\sim 37,000$ km² area of the

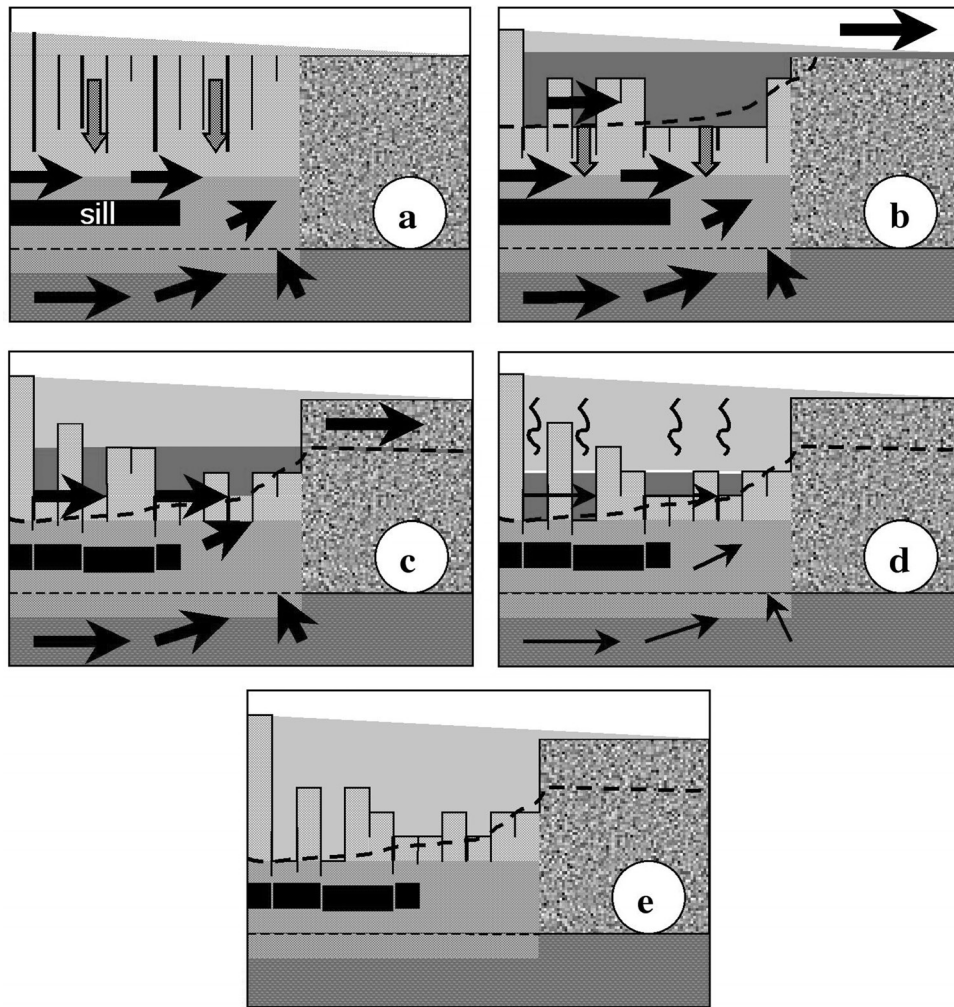


Figure 9. (a) Emplacement of a large sill (accompanied by at least one feeder dike, not shown, from Eastern Tharsis) causes fracturing (vertical lines) of the surrounding cryosphere. This initiates thawing of ice. Subsidence and piecemeal collapse of the cryosphere above and around the hot magma in the sill and dikes begin (checkered arrows). Water begins to rise from the pressurized aquifer below the cryosphere (arrow size represents water flux). (b) Subsidence (checkered gray arrows) forms the Aromatum Chaos depression (average floor position indicated by dashed line) which fills with water. The water overtops the highest part of the floor at the eastern end of Aromatum Chaos and begins to erode the channel of Ravi Vallis. (c) Aromatum Chaos continues to be eroded and deepened by heat from the magma thawing the cryosphere and water carrying away sediment. The outlet at the eastern end is eroded down by water outflow and the Ravi Vallis channel becomes deeper. Displacements within the melting cryosphere allow multiple fractures to penetrate the sill itself, greatly facilitating water rise. (d) The amount of water released from the aquifer now decreases because of the drawdown of the water level in Gangis Chasma. Erosion of the depression rapidly declines as the amount of water released becomes less than the amount of water vapor escaping into the atmosphere. Overflow into Ravi Vallis ceases and ice-covered water ponds in the depression. The magma in the sill and dikes solidifies, and the last stages of heat release cause minor subsidence of cryosphere blocks. Eventually all the water in Aromatum Chaos freezes and the ice progressively sublimates. (e) The fractured cryosphere has now frozen again and all of the ponded water ice has sublimated. The height of the lip of the floor at the eastern end of the depression is ~ 1.2 km below the preintrusion surface level and the deepest part of the depression is ~ 3.45 km.

triangular region to the west of Aromatum Chaos showing signs of incipient subsidence, making it a candidate source area. For smaller sediment-bearing capacities the required area is proportionately larger. Even allowing for the possi-

bility that the porosity of the aquifer was significantly greater than the $\sim 3\%$ assumed, this strongly suggests that Gangis Chasma was the main source of the water feeding the Aromatum-Ravi and Shalbatana channel systems.

[39] **Acknowledgments.** L.W. and K.L.M. were supported by PPARC grant PPA/G/S/2000/00521. K.L.M. also acknowledges support by the NRC in the form of a Postdoctoral Research Associateship, carried out at the Jet Propulsion Laboratory, California Institute of Technology, under a contract with the National Aeronautics and Space Administration. We thank J. W. Head for useful discussions and D. McKenzie and C. Hamilton for their helpful reviews.

References

- Baker, V. R., and R. C. Kochel (1979), Martian channel morphology: Maja and Kasei Valles, *J. Geophys. Res.*, *84*(B14), 7961–7983.
- Baker, V. R., R. G. Strom, V. C. Gulick, J. S. Kargel, G. Komatsu, and V. S. Kale (1991), Ancient oceans, ice sheets and the hydrological cycle on Mars, *Nature*, *352*, 589–594.
- Burr, D. M. (2003), Temporary ponding of floodwater in Athabasca Vallis, Mars, *Lunar Planet. Sci.* [CD-ROM], XXXIV, Abstract 1066.
- Burr, D. M., A. S. McEwen, and S. E. H. Sakimoto (2002a), Recent aqueous floods from the Cerberus Fossae, *Geophys. Res. Lett.*, *29*(1), 1013, doi:10.1029/2001GL013345.
- Burr, D. M., J. A. Grier, A. S. McEwen, and L. P. Keszthelyi (2002b), Repeated aqueous flooding from the Cerberus Fossae: Evidence for very recently extant, deep groundwater on Mars, *Icarus*, *159*(1), 53–73.
- Burr, D. M., A. S. McEwen, L. P. Keszthelyi, and P. D. Lanagan (2002c), Extensive aqueous flooding from the Cerberus Fossae, Mars, and its implications for the Martian hydrosphere, *Lunar Planet. Sci.* [CD-ROM], XXXIII, Abstract 1047.
- Busche, D. (2001), Early Quaternary landslides of the Sahara and their significance for geomorphic and climatic history, *J. Arid Environ.*, *49*, 429–448.
- Cabrol, N. A., E. A. Grin, and G. Dawidowicz (1997), A model of outflow generation by hydrothermal under pressure drainage in volcano-tectonic environment, Shalbatana Vallis (Mars), *Icarus*, *125*, 455–464.
- Carr, M. H. (1979), Formation of Martian flood features by release of water from confined aquifers, *J. Geophys. Res.*, *84*(B6), 2995–3007.
- Carr, M. H. (1990), D/H on Mars: Effects of floods, volcanism, impacts and polar processes, *Icarus*, *87*, 210–227.
- Carr, M. H., R. Greeley, K. R. Blasius, J. E. Guest, and J. B. Murray (1977), Some Martian volcanic features as viewed from the Viking orbiters, *J. Geophys. Res.*, *82*(28), 3985–4015.
- Carslaw, H. S., and J. C. Jaeger (1947), *Conduction of Heat in Solids*, 386 pp., Oxford Univ. Press, New York.
- Chapman, M. G., and D. H. Scott (1989), Geology and hydrology of the North Kasei Valles area, Mars, *Proc. Lunar Planet. Sci. Conf.*, *19th*, 367–375.
- Chapman, M. G., and K. L. Tanaka (1990), Small valleys and hydrologic history of the lower Mangala Valles region, Mars, *Proc. Lunar Planet. Sci. Conf.*, *20th*, 531–539.
- Chapman, M. G., and K. L. Tanaka (2002), Related magma-ice interactions: Possible origins of chasmata, chaos, and surface materials in Xanthe, Margaritifer, and Meridiani Terrae, Mars, *Icarus*, *155*, 324–339.
- Chapman, M. G., M. T. Gudmundsson, A. J. Russell, and T. M. Hare (2003), Possible Juventae Chasma subice volcanic eruptions and Maja Valles ice outburst floods on Mars: Implications of Mars Global Surveyor crater densities, geomorphology, and topography, *J. Geophys. Res.*, *108*(E10), 5113, doi:10.1029/2002JE002009.
- Clifford, S. M. (1993), A model for the hydrologic and climatic behavior of water on Mars, *J. Geophys. Res.*, *98*(E6), 10,973–11,016.
- Coleman, N. M. (2002), No mystery! Water carved the outflow channels on Mars, *Eos. Trans. AGU*, *83*(47), Fall Meet. Suppl., Abstract P51B-0362P51B-0362.
- Coleman, N. M. (2003), Aqueous flows carved the outflow channels on Mars, *J. Geophys. Res.*, *108*(E5), 5039, doi:10.1029/2002JE001940.
- Coleman, N. M. (2004), Ravi Vallis, Mars-paleoflood origin and genesis of secondary chaos zones, *Lunar Planet. Sci.* [CD-ROM], XXXV, Abstract 1299.
- Coleman, N. M., and C. L. Dinwiddie (2005), Groundwater depth, cryosphere thickness, and crustal heat flux in the epoch of Ravi Vallis, Mars, *Lunar Planet. Sci.* [CD-ROM], XXXVI, Abstract 2163.
- Coleman, J. M., D. B. Prior, and L. E. Garrison (1978), Submarine landslides in the Mississippi river delta, *Proc. Offshore Technol. Conf.*, *10th*, 1067–1074.
- Costa, J. E. (1988), Rheologic, geomorphic, and sedimentologic differentiation of water floods, hyperconcentrated flows, and debris flows, in *Flood Geomorphology*, edited by V. R. Baker et al., pp. 113–122, John Wiley, Hoboken, N. J.
- Department of Scientific and Industrial Research (1964), *Steam Tables 1964*, Natl. Eng. Lab., H. M. Stn. Off., Edinburgh, U. K.
- Dohm, J. M., et al. (2001), Latent outflow activity for Western Tharsis, Mars: Significant flood record exposed, *J. Geophys. Res.*, *106*(E6), 12,301–12,314.
- Formisano, V., S. Atreya, T. Encrenaz, N. Ignatiev, and M. Giuranna (2004), Detection of methane in the atmosphere of Mars, *Science*, *306*, 1758–1761.
- Gilmore, M. S., and E. L. Phillips (2002), Geologic control of gully depths in three regions of Mars, *Lunar Planet. Sci.* [CD-ROM], XXXIII, Abstract 1295.
- Greeley, R., and P. D. Spudis (1981), Volcanism on Mars, *Rev. Geophys.*, *19*(1), 13–41.
- Hanna, J. C., and R. J. Phillips (2003), A new model of the hydrologic properties of the Martian crust and implications for the formation of valley networks and outflow channels, *Lunar Planet. Sci.* [CD-ROM], XXXIV, Abstract 2027.
- Hanna, J. C., and R. J. Phillips (2005), Hydrological modeling of the Martian crust with application to the pressurization of aquifers, *J. Geophys. Res.*, *110*, E01004, doi:10.1029/2004JE002330.
- Head, J. W., and L. Wilson (2001), Mars: Geological setting of magma/H₂O interactions, *Lunar Planet. Sci.* [CD-ROM], XXXII, Abstract 1215.
- Head, J. W., and L. Wilson (2002), Mars: A review and synthesis of general environments and geological settings of magma-H₂O interactions, in *Volcano-Ice Interaction on Earth and Mars*, edited by J. L. Smellie and M. G. Chapman, *Geol. Soc. London Spec. Publ.*, *202*, 27–57.
- Head, J. W., L. Wilson, and K. L. Mitchell (2003), Generation of recent massive water floods at Cerberus Fossae, Mars by dike emplacement, cryospheric cracking, and confined aquifer groundwater release, *Geophys. Res. Lett.*, *30*(11), 1577, doi:10.1029/2003GL017135.
- Hoffman, N. (2000), White Mars: A new model for Mars' surface and atmosphere based on CO₂, *Icarus*, *146*(2), 326–342.
- Hoffman, N. (2001), Explosive CO₂-driven source mechanisms for an energetic outflow “jet” at Aromatum Chaos, Mars, *Lunar Planet. Sci.* [CD-ROM], XXXII, Abstract 1257.
- Kochel, R. C., and J. F. Piper (1986), Morphology of large valleys on Hawaii: Evidence for groundwater sapping and comparisons with Martian valleys, *Proc. Lunar Planet. Sci. Conf. 17th*, Part 1, *J. Geophys. Res.*, *91*(B13), suppl., E175–E192.
- Komar, P. D. (1980), Modes of sediment transport in channelized water flows with ramifications to the erosion of the Martian outflow channels, *Icarus*, *42*, 317–329.
- Kuzmin, R. O., R. Greeley, and D. M. Nelson (2002), Mars: The morphological evidence of late Amazonian water activity in Shalbatana Vallis, *Lunar Planet. Sci.* [CD-ROM], XXXIII, Abstract 1087.
- Laity, J. E., and M. C. Malin (1985), Sapping processes and the development of theater-headed valley networks on the Colorado Plateau, *Geol. Soc. Am. Bull.*, *96*, 203–217.
- Lane, M. D., M. D. Dyar, and J. L. Bishop (2004), Spectroscopic evidence for hydrous iron sulphate in the Martian soil, *Geophys. Res. Lett.*, *31*, L19702, doi:10.1029/2004GL021231.
- Leask, H. J. (2005), Volcano-ice interactions and related geomorphology at Mangala Valles and Aromatum Chaos, Mars, M.Ph. thesis, 199 pp., Lancaster Univ., Lancaster, U. K.
- Leask, H. J., L. Wilson, and K. L. Mitchell (2004), The formation of Aromatum Chaos and the water discharge rate at Ravi Vallis, *Lunar Planet. Sci.* [CD-ROM], XXXV, Abstract 1544.
- Leask, H. J., L. Wilson, and K. L. Mitchell (2006), Formation of Ravi Vallis outflow channel, Mars: Morphological development, water discharge, and duration estimates, *J. Geophys. Res.*, *111*, E08070, doi:10.1029/2005JE002550.
- Lucchitta, B. K., N. K. Isbell, and A. Howington-Kraus (1994), Topography of Valles Marineris: Implications for erosional and structural history, *J. Geophys. Res.*, *99*(E2), 3783–3798.
- Luo, W., R. E. Arvidson, M. Sultun, R. Becker, M. K. Crombie, N. Sturchio, and Z. El Alfy (1997), Ground-water sapping processes, western desert, Egypt, *Geol. Soc. Am. Bull.*, *109*(1), 43–62.
- Mars Channel Working Group (1983), Channels and valleys of Mars, *Geol. Soc. Am. Bull.*, *94*, 1035–1054.
- Masursky, H., J. M. Boyce, A. L. Dial, G. G. Schaber, and M. E. Strobil (1977), Classification and time of formation of Martian channels based on Viking data, *J. Geophys. Res.*, *82*(28), 4016–4038.
- Max, M. D., and S. M. Clifford (2001), Initiation of Martian outflow channels: Related to the dissociation of gas hydrate?, *Geophys. Res. Lett.*, *28*(9), 1787–1790.
- McGovern, P. J., S. C. Solomon, D. E. Smith, M. T. Zuber, M. Simons, M. A. Wieczorek, R. J. Phillips, G. A. Neumann, O. Aharonson, and J. W. Head (2002), Localized gravity/topography admittance and correlation spectra on Mars: Implications for regional and global evolution, *J. Geophys. Res.*, *107*(E12), 5136, doi:10.1029/2002JE001854.
- McKenzie, D., and F. Nimmo (1999), The generation of Martian floods by the melting of ground ice above dykes, *Nature*, *397*, 231–233.
- Moore, J. M., G. D. Clow, W. L. Davis, V. C. Gulick, D. R. Janke, C. P. McKay, C. R. Stoker, and A. P. Zent (1995), The circum-Chryse region as

- a possible example of a hydrologic cycle on Mars: Geologic observations and theoretical evaluation, *J. Geophys. Res.*, *100*(E3), 5433–5447.
- Mouginis-Mark, P. J. (1985), Volcano/ground ice interactions in Elysium Planitia, Mars, *Icarus*, *64*, 265–284.
- Mouginis-Mark, P. J. (1990), Recent water release in the Tharsis region of Mars, *Icarus*, *84*, 362–373.
- Mouginis-Mark, P. J., L. Wilson, J. W. Head, S. H. Brown, J. L. Hall, and K. D. Sullivan (1984), Elysium Planitia, Mars: Regional geology, volcanology, and evidence for volcano-ground ice interactions, *Earth Moon Planets*, *30*, 149–173.
- Nelson, D. M., and R. Greeley (1999), Geology of Xanthe Terra outflow channels and the Mars Pathfinder landing site, *J. Geophys. Res.*, *104*(E4), 8653–8669.
- Nummedal, D., and D. B. Prior (1981), Generation of Martian chaos and channels by debris flows, *Icarus*, *45*, 77–86.
- Palmero, A., S. Sasaki, R. O. Kuzmin, and R. Greeley (2003), Formation and sources of the Shalbatana valley system, *Lunar Planet. Sci.* [CD-ROM], *XXXIV*, Abstract 1062.
- Rodriguez, J. A. P., S. Sasaki, and H. Miyamoto (2003), Nature and hydrological relevance of the Shalbatana complex underground cavernous system, *Geophys. Res. Lett.*, *30*(6), 1304, doi:10.1029/2002GL016547.
- Rotto, S., and K. L. Tanaka (1995), Geologic/geomorphologic map of the Chryse Planitia region of Mars, *U.S. Geol. Surv. Misc. Invest. Map*, *I-2441*.
- Schultz, P. H., R. A. Schultz, and J. Rogers (1982), The structure and evolution of ancient impact basins on Mars, *J. Geophys. Res.*, *87*(B12), 9803–9820.
- Scott, D. H., and K. L. Tanaka (1986), Geologic map of the western equatorial region of Mars, *U.S. Geol. Surv. Misc. Invest. Map*, *I-1802-A*.
- Scott, E. D., and L. Wilson (1999), Evidence for a sill emplacement on the upper flanks of the Ascracus Mons shield volcano, Mars, *J. Geophys. Res.*, *104*(E11), 27,079–27,089.
- Sharp, R. P. (1973), Mars: Fretted and chaotic terrains, *J. Geophys. Res.*, *78*(20), 4073–4083.
- Sharp, R. P., L. A. Soderblom, B. C. Murray, and J. A. Cutts (1971), The surface of Mars: 2. Un cratered terrains, *J. Geophys. Res.*, *76*(2), 331–342.
- Smith, G. A. (1986), Coarse-grained nonmarine volcanoclastic sediment: Terminology and depositional process, *Geol. Soc. Am. Bull.*, *97*, 1–10.
- Squyres, S. W. (1984), The history of water on Mars, *Annu. Rev. Earth Planet. Sci.*, *12*, 83–106.
- Squyres, S. W., D. E. Wilhelms, and A. C. Mooseman (1987), Large-scale volcano-ground ice interactions on Mars, *Icarus*, *70*, 385–408.
- Squyres, S. W., S. M. Clifford, R. O. Kuzmin, J. R. Zimbleman, and F. M. Costard (1992), Ice in the Martian regolith, in *Mars*, edited by H. H. Kieffer et al., chap. 16, pp. 523–554, Univ. of Ariz. Press, Tucson.
- Stewart, S. T., and F. Nimmo (2001), Surface runoff features on Mars: Testing the carbon dioxide formation hypothesis, *Lunar Planet. Sci.* [CD-ROM], *XXXII*, Abstract 1780.
- Tanaka, K. L. (1999), Debris-flow origin for the Simud/Tiu deposit on Mars, *J. Geophys. Res.*, *104*(E4), 8637–8652.
- Tanaka, K. L., J. M. Dohm, J. H. Lias, and T. M. Hare (1998), Erosional valleys in the Thaumasia region of Mars: Hydrothermal and seismic origins, *J. Geophys. Res.*, *103*(E13), 31,407–31,419.
- Tanaka, K. L., J. S. Kargel, D. J. MacKinnon, T. M. Hare, and N. Hoffman (2002), Catastrophic erosion of Hellas basin rim on Mars induced by magmatic intrusion into volatile-rich rocks, *Geophys. Res. Lett.*, *29*(8), 1195, doi:10.1029/2001GL013885.
- Theilig, E., and R. Greeley (1979), Plains and channels in the Lunae Platum–Chryse Planitia region of Mars, *J. Geophys. Res.*, *84*(B14), 7994–8010.
- Urquart, M. L., and V. C. Gulick (2003), Plausibility of the “white Mars” hypothesis based upon the thermal nature of the Martian subsurface, *Geophys. Res. Lett.*, *30*(12), 1622, doi:10.1029/2002GL016158.
- Wilhelms, D. E., and R. J. Baldwin (1989), The role of igneous sills in shaping the Martian uplands, *Proc. Lunar Planet. Sci. Conf.*, *19th*, 355–367.
- Wilson, L., and J. W. Head (2002), Volcano eruption styles on Mars due to shallow interactions between magma and volatiles, *Lunar Planet. Sci.* [CD-ROM], *XXXIII*, Abstract 1275.
- Wilson, L., and P. J. Mouginis-Mark (2003), Phreatomagmatic explosive origin of Hrad Vallis, Mars, *J. Geophys. Res.*, *108*(E8), 5082, doi:10.1029/2002JE001927.

H. J. Leask and L. Wilson, Planetary Science Research Group, Environmental Science Department, Institute of Environmental and Natural Sciences, Lancaster University, Lancaster LA1 4YQ, UK. (l.wilson@lancaster.ac.uk)

K. L. Mitchell, Jet Propulsion Laboratory, MS 183-601, 4800 Oak Grove Drive, Pasadena, CA 91109-8099, USA.